Stability behavior of chemically synthesized organic electrolyte salts and methylammonium lead halide perovskite light harvester

Rajan Kumar Singh, Neha Jain, Jai Singh, Ranveer Kumar[*]

Department of Physics, School of Mathematical and Physical Sciences, Dr. Harisingh Gour Central University, Sagar, 470003, Madhya Pradesh, India

[*]Corresponding author, Tel: (+ 91) 9425635731; E-mail: ranveerionics@gmail.com

Abstract

This is the first time that a highly purified white organic electrolyte salts (OES), Methylammonium iodide, CH_3NH_3I (MAI) and Methylammonium chloride, CH_3NH_3Cl (MACl) have been successfully synthesized by a new technique, high vacuum oven evaporation method (HVOE), which is inexpensive and less time consumable. Thermal stability of organic salt, pure and mixed perovskite light harvester materials (PLHM) are studied by STA (DTG/DTA). CH_3NH_3I and CH_3NH_3Cl undergo ~100% weight loss in one step, at temperature 310°C and 350°C, respectively. Additionally, $CH_3NH_3PbI_3$ is more thermally stable than mixed halide perovskite $CH_3NH_3PbI_{3-x}Cl$. Stability behavior of organic salts and $CH_3NH_3PbI_{3-x}Cl_x$ is analyzed by Raman study which indicates that organic salts are stable in ambient conditions and $CH_3NH_3PbI_{3-x}Cl_x$ is not stable in ambient condition. Different stretching and banding modes of organic and inorganic materials are indentified by study of Raman spectra. Copyright © 2017 VBRI Press.

Keywords: Organic electrolyte salt, perovskite, light harvester, stability, DTA/DTG, Raman.

Introduction

Methylammonium lead halide perovskite $CH_3NH_3PbX_3$ (X = Cl, Br, or I) material is one of the most improving light harvesters due to its a strong optical absorption, an adjustable band gap, long diffusion length [1-4] high carrier mobility, low defect density [5], small excitation binding energies [6, 7] and low recombination rate [8]. Besides, these properties perovskite light harvesters show ambipolar charge transport nature i.e. acts as electron as well as hole transporting material [9]. In addition, ambipolar charge transport nature of perovskite materials help in developing high-efficient photovoltaic devices. Thus, due to this behavior, perovskite material can be used for development of solar cell device without mesoporous oxide [10-12] and in some another case without hole transporting layers [13, 14]. Most of the hybrid perovskite material is used for high efficient photovoltaic solar cell and recently it is also used as photo detector, [15, 16] light emitting diodes [17], random access memory [18, 19], amplifier achieve device [20], tunable electrically pumped Lasers [21] and water splitting devices [22, 23]. Most recently, organic-inorganic halide perovskite material can also be used for detection of X-ray [24], photons and ultraviolet rays which have promising application in ultrafast, non-linear devices, optothermal detections, computer memories, and

biocompatible optoelectronic probes and in other medical diagnosis [25, 26]. Due to unique properties and huge applications of perovskite material in solar cell it is trending topic for scientists and a lot of research is being carried out at present. Within only five years the efficiency of perovskite based solar cell reached from 3.8% to 20.1% which shows the rapid increase in efficiency and interest of research community [26]. In 2009, first organic-inorganic halide perovskite material ($CH_3NH_3PbI_3$ and $CH_3NH_3PbBr_3$) was developed for photoelectron chemical cell by Miyasaka group with power conversion efficiency (PCE) of 3.81% [26]. After that Park et al. fabricated solar cell using $CH_3NH_3PbI_3$ in 2011 with PCE 6.54% [27]. At the end of 2014, Yang group achieved 19.3% efficiency by doping of Yttrium with TiO_2 and NREL certified a highest PCE of 20.1% solar cell, based on organic-inorganic halide perovskite harvester [28, 29].

In most of the cases, $CH_3NH_3PbI_3$ material has given good device performance with mesoporous structured architecture and $CH_3NH_3PbI_{3-x}Cl_x$ material gives high efficiency with planer architectures [30]. Currently material/ device stability is the key issue for the applications of PLHMs in different fields. PLHMs are quite sensitive to moisture and oxygen that's why most of the fabrication process conducted inside a glove box. Thermal behavior of OES and perovskite materials also

affects the performance and stability of devices. Stability of OES and PLHMs can be improved by new synthesis techniques so that, it can be transferred from the laboratory to industry and outdoor applications.

In this work, we focused on the role of different halide (Cl and I) electrolyte salts as precursors for the formation of pure and mixed halide perovskite light harvester. We studied the thermal behavior of different halide electrolyte salts and their corresponding perovskite material which helps to clarify the role of different electrolyte salts used in perovskite materials. Vibrational features, crystallinty and stability of perovskite are studied by Raman spectroscopy. To the best of our knowledge, it is first time reported the production of MAI and MACl without rotatory evaporator and further long purification process with diethyl ether. We have developed a new HVOE technique that can overcome problem of impurities in electrolyte salt and make it stable in ambient conditions. Additionally, this method also increases the thermal stability of electrolyte salts and PLHMs. Bulk amount of PLHMs are obtained by wet chemical process which helps in the commercialization and bulk mass production of hybrid perovskite powder.

Experimental methods

MAI and MACl salts are prepared by mixing 15 ml hydriodic acid (53% in water) (Merck, India) and 15 ml hydrochloric acid (57% in water Fisher scientific, India), respectively with 14 ml methylamine (40% in methanol, Sigma Aldrich, USA), in a 250 ml round – bottomed flask under continuous stirring at 0°C for 2 hrs. This process should be handling with care due to exothermic reaction. MAI and MACl solutions are crystallized by removing the solvent in high vacuum oven (JEIO, TECH OV-11/12) at 60°C for 24 hrs. White precipitate is formed after drying in vacuum; this powder is grinded in agate mortal pestle which gives fine white salt. This can be stored for long time by keeping it in glove box or in dry place.

For the synthesis of $CH_3NH_3PbI_3$ perovskite, we mixed as prepared MAI and PbI_2 (99% Sigma Aldrich, USA) with 1:1 molar ratio in N, N'- dimethyleformamide (DMF) (99.8% Sigma Aldrich, USA) by stirring at 60°C for 6hrs. A transparent yellowish homogeneous solution is obtained which is used as precursor for device formation. To obtain the $CH_3NH_3PbI_3$ in powder form, we put the solution to dry in vacuum oven at 100°C for 6hrs. Black fine powder is obtained by grinding in agate mortar pestle. Due to high sensitivity of prepared sample towards moisture and oxygen this prepared sample is stored in nitrogen filled glove box.

$CH_3NH_3PbI_{3-x}Cl_x$ is obtained by mixing prepared, MAI and $PbCl_2$ (>98% Merck, Germany) with 3:1 molar ratio in DMF solvent (99.8% Sigma Aldrich, USA) with stirring at 60^0 C for 12hrs. A light yellow homogeneous solution is obtained and after dried in vacuum oven at 100^0 C for 5 hrs, we obtained black $CH_3NH_3PbI_{3-x}Cl_x$ powder. This is also highly sensitive to humidity, so it is stored it in N_2 filled glove box.

TG-DTA of different perovskite material and electrolyte salts was simultaneously carried out on NETZCH STA 449 F1 Jupiter. Materials were placed in an alumina crucible and heated at a rate of 10 °C min^{-1} from room temperature 23 °C to 500 °C for electrolyte salts and up to 600^0C for perovskite materials under N_2 atmosphere gas flowing with rate of 60ml/min. Raman spectra of samples are characterized by a micro spectroscopic Raman setup (RENISHAW) using He-Ne (633nm) laser source for excitation of molecules. All the samples were measured at room temperature and ambient air.

Results and discussion

TG measurement of electrolyte salt MAI and MACl shows a rapid 100% mass loss between 275 to 370^0C and 250 to 350^0C, respectively and both of them undergo sublimation process at sublimation temperature of 250 and 210 ^{0}C for MAI and MACl, respectively which is quite higher than previous reported results without complex decomposition **[31-33]** as shown in **Fig. 1(a)** and **(b).**These results suggested that, new preparation technique of organic salts makes it more stable than by traditional methods.TG result also confirms that the release of CH_3NH_3I occurs at higher temperature while lower onsets of the weight loss temperature of CH_3NH_3Cl suggest that it is easier to turn into gaseous phase. Additionally, MAI is more thermally stable than MACl due to higher sublimation temperature than Cl containing organic salt. DTA graphs, as inset **Fig. 1(a)** and **(b)** shows the three endothermic peaks for MAI and two small endothermic peaks of MAI which shows the solid- solid phase transition, producing a metastable pre-melting state without any mass loss while in MACl there is only one pre-melting state at 235.7 ^{0}C. An instance and sharp endothermic peak is observed at 370 ^{0}C for MAI and at 347.2 ^{0}C for MACl which indicates the melting point of the respective salts.
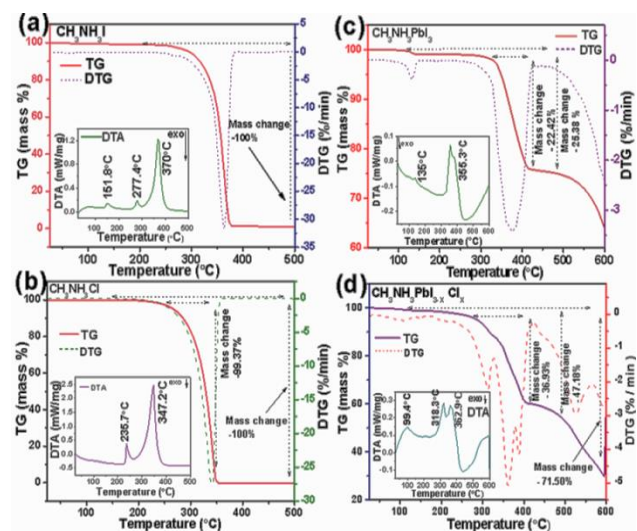

Fig. 1. DTA/DTG curve of organic electrolyte salts (CH_3NH_3I and CH_3NH_3Cl) and perovskite light harvesters ($CH_3NH_3PbI_3$ and $CH_3NH3PbI_{3-x}Cl_x$) measured at 10^0C min^{-1} under N_2 (a) TG curve of

MAI with 100% mass loss at 370°C and dotted line shows, 1st derivative of TG curve. Inset figure shows the DTA curve of MAI with three endothermic peaks at 151°C, 277°C and 370°C (b) TG curve of MACl undergo 100% mass loss at 350°C and DTA curve shows two endothermic peaks at 235°C and 347.2°C in inset figure. (c) TG curve of $CH_3NH_3PbI_3$ and doted curve shows 1st derivative of TG curve and inset figure is for DTA. (d) TG curve of $CH_3NH_3PbI_{3-x}Cl_x$ and doted curve shows 1st derivative of TG curve and inset figure is for DTA with three endothermic peaks.

From the DTG curve of $CH_3NH_3PbI_{3-x}Cl_x$ & $CH_3NH_3PbI_3$ as shown in **Fig. 1(c)** and **(d),** it is clear that pure iodide containing perovskite is more thermally stable than Cl containing ($CH_3NH_3PbI_{3-x}Cl_x$) perovskite, because MAI salt is more stable than MACl as discussed above. Perovskite materials are stable up to 300 ^{0}C after that $CH_3NH_3PbI_{3-x}Cl_x$ and $CH_3NH_3PbI_3$ materials, undergo 36.93%, and 22.42%, weight loss of HCl & HI respectively at 420 ^{0}C and another 10.25% mass loss of CH_3NH_2 occur at 500 ^{0}C.

These results are indicating that the active group (amine) can be more firmly bound to perovskite structure as compared to HCl and HI of their respective perovskite materials. This type of decomposition is not observed in the pure MAI and MACl, which shows that this type of decomposition behavior occurs only when the organic species are incorporated in to the perovskite structure. Additionally, further increase of temperature, mass loss of perovskite also increases due to decomposition of inorganic material, PbI_2 and $PbCl_2$ because lead iodide and lead chloride undergo 96.01% and 92.04% mass loss up to 800 °C.

Inset figures of **Fig. 1(c)** and **(d)** shows the DTA curve of perovskite which reveals that there are two endothermic peaks at 135 and 355 ^{0} C for $CH_3NH_3PbI_3$ and three endothermic peaks for $CH_3NH_3PbI_{3-x}Cl_x$ at 99.4, 318.3 and 362.9^{0}C. These peaks demonstrate that mixed perovskite might decompose into 3 steps while pure iodine containing perovskite decompose into only 2 steps. Thus, from TG/DTA study of **Fig. 1**, we may have concluded that perovskite material seem to be more stable at higher temperature than their corresponding organic electrolyte & structure because there is no mass loss at their respective sublimation temperature and stability of perovskite also depends on anions present in it.

Fig. 2(a) shows the Raman spectra of CH_3NH_3I organic salt. At ambient condition MAI shows, well known Raman bands at ~110, 985, 1457, 1539, 2958 and 3090 cm^{-1} and weak bands near 94, 1400 & 2900 cm^{-1}. Strong band appears due to stretching and bonding of ions present in the organic salt. 110 cm^{-1} band shows the lattice vibration in the crystal internal vibrational modes of CH_3NH_2 appears at high frequency around 914 and 985 cm^{-1} which due to C-N stretching and medium Raman bands between (1400-1550 cm^{-1}) occurs due to CH_3 and NH_3 stretching **[34, 35]**. **Fig. 2(b)** and **(c)** show the Raman spectra of CH_3NH_3I from which we check the stability of salt with different time durations (0 to 95 days).

From these spectra, it is found that there are no changes in any band up to 95 days after synthesis which indicates the stability of MAI as well as MACl. **Fig. 2(d)**

shows the Raman spectra of MACl salt with strong Raman bands at 77, 994 and 2960 cm^{-1}, some medium bands at 1300 cm^{-1} and 1550 cm^{-1} and weak bands at 1900 cm^{-1} and 2828 cm^{-1}. In addition, to this MAI, MACl also shows a strong Raman band near 994 cm^{-1} due to the C-N stretching. There is additional medium band near 1300 cm^{-1} due to the CH_3 bending which is not present in MAI. Other bands between 1400 - 1550 cm^{-1} is nearly same as MAI due to CH_3NH_3 bending present in sample. Few medium and strong peaks appear at 2828 cm^{-1} and 2960 cm^{-1}, indicates the presence of CH_3NH_2 and HCl stretching in the sample. **Fig. 2(e)** and **(f)** indicates that MACl which is also stable in ambient condition and there is no degradation in material.
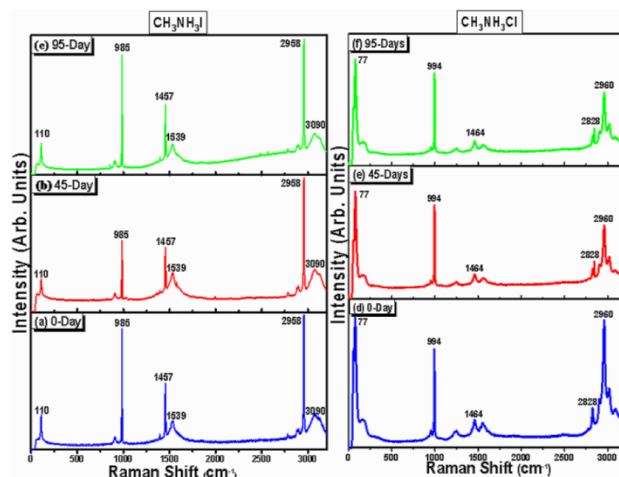

Fig. 2. Raman spectra of organic electrolyte salt CH_3NH_3I **(a)** synthesized at same day **(b)** after 45 days **(c)** after 95 days. Raman spectra of electrolyte salt CH_3NH_3Cl **(d)** synthesized at same day **(e)** after 45 days **(f)** after 95days.

The Raman spectra of $CH_3NH_3PbI_{3-X}Cl_x$ with different time duration are given in **Fig. 3**. There are around four different Raman Vibrational peaks at 53, 65, 77 and 100 cm^{-1} and one additional broader small peak -170cm^{-1} present in $CH_3NH_3PbI_{3-X}Clx$ perovskite material. These peaks are attributed to the Perovskite layers, especially bends of Pb-I and Pb-Cl in mixed halide Perovskite light harvester **[36]**.

Band near 65 cm^{-1} indicate the presence of inorganic components which is confirmed by previous studies on related perovskite material **[37]** and weak bands at 170 cm^{-1} indicates presence of MA organic cation **[38].** Thus, from Raman spectra of materials, it is confirmed that synthesized hybrid perovskite material, consists of organic and inorganic components. The study of perovskite spectra in different time intervals indicate that intensity of Raman bands decreases, which indicate degradation of material in ambient condition. Organic bands degrade in few hours and inorganic bends degrades slower than organic bends. The Raman study of MAI, MACl and perovskite material the details of structure and Vibrational property of the different perovskite materials as well as their corresponding electrolyte salt can be easily understood and it can be also useful in study the tuning of different depends in perovskite materials.
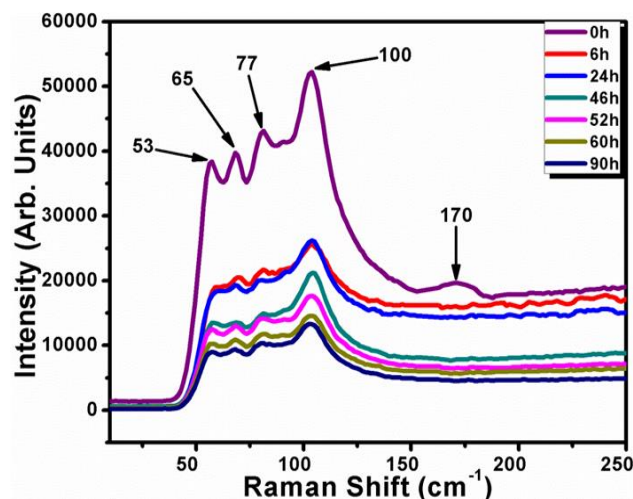

Fig. 3. Raman spectra of mixed halide, CH$_3$NH$_3$PbI$_{3-x}$Cl$_x$ perovskite light harvesting　material for different time period of 0 hrs to 90 hrs in ambient condition. Intensity of peaks is decreases with time duration due to moisture and ambient air.

Conclusion

MAI and MACl electrolyte salts have been successfully synthesized with new method i.e. HVOE technique. In addition, PLHMs are synthesized by wet chemical synthesis method. This new technique, improves the stability of OES and PLHMs which helps in bulk production of light harvesting material which is beneficial for commercialization of organic salts and harvesting materials. Thus, future of PLHMs is looking bright as highly efficient photovoltaic cells **[39-42]** and it has many new applications as a color convertor for visible light communication **[43],** in Li–ion batteries **[44]** and in other optoelectronic applications **[45].** DTG study of organic salt reveals that MAI is more thermally stable than MACl and both get 100% mass loss at temperature 370 and 350 ^{0}C, respectively and DTA shows endothermic nature in both salts. DTG curve of CH$_3$NH$_3$PbI$_3$ and of CH$_3$NH$_3$PbI$_{3-X}$Cl$_x$ confirms that higher annealing temperature required for the MAI/ PbI$_2$ precursor mixture. Raman spectra of perovskite material show the presence of organic- inorganic bands. By the stability testing at different time period of salts, concluded that electrolyte salt does not degrade in ambient condition so there is no need to store in globe box or vacuum desiccators, whereas perovskite material starts degrading within few hours in ambient condition.
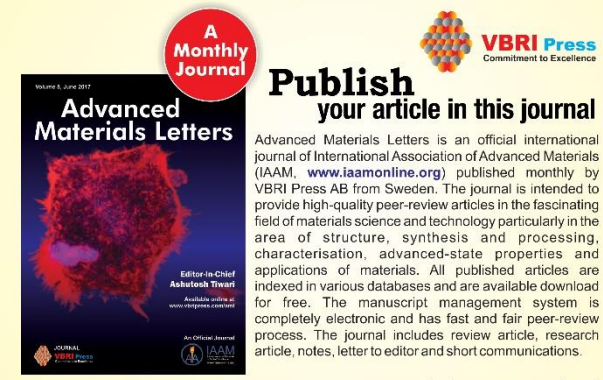
References

1. Xing G, Mathews N.; Sun S.; Lim S.S.; Lam Y.M.; Gratzel M; Mhaisalkar S.; Sum T.C. *Science*, **2013**, 7, 342-344.

DOI: 10.1126/science.1243167
2. Stanks S.D.; Eperon G.E.; Grancini G.; Menelaou C.; Alcocer M. J. P.; Leijtens T.; L.M., Petrozza A; Snaith H.J.; *Science,* **2013**, *342*, 341-344.
DOI: 10.1126/science.1243982.
3. Aharon S. and Etgor L.; *Nano Let,* **2016**, *16*, 3230-3235.
DOI: 10.1021/acs.nanolett.6b00665
4. Bhaumik S.; Veldhuis S. A.; Ng Y. F.; Li M.; Muduli S. K.; Chien T.; Damodaram B.;Nhaisalkar S. and Mathews N.; Chem. Commun, **2016**, *52*, 7118-7121.
DOI: 10.1039/c6cc01056c
5. Xing G; Mathews N.; Lim S.S.; Yantara N.; Liu X.; Sabba D.; GratZel M.; Mhaisalkar S.; Sum T.C.; *Nat. Mater,* **2014**,*13*,476-480.
DOI: 10.1038/nmat3911.
6. Ishiharat T. J., Lumin., **1994**, 61, 269.
DOI: 10.1016/0022-2313(94)90145-7
7. Sun S., Salim T.; Mathiws N.; Duchamp M.; Boothroyd C.; Xing G.; Sum T.C.; Lam Y.M., *Energy Environ. Science,* **2014**, 7, 399-407.
DOI: 10.1039/C3EE43161D
8. Wehrenfenning C.; Eperon G.E.; Johnston M.B.; Snaith H.J.; Herz L.M., *Avd. Mater,* **2014**, *26*, 1584-1589.
DOI: 10.1002/adma.201305172
9. Heo J.H.; Im S.H.; Noh J.H.; Mandal T.N.; Lim C.S.; Chan J.A.; Lee Y.H.; Kim H.J.; Sarkar A.; Nazeeruddin M.K.; Gratzel M. and Seok S.I., , *Nat. photonics*, **2013**, 7, 486-491.
DOI: 10.1038/nphoton.2013.80
10. Kim H-S; Lee C-R; Im J-H; Lee K.B.; Moehl T.; Marchiovo A.; Moon S.J.; Baker R. H.; Yam J.H.; Moser J.E.; Gratzel M. and N.G., *Sci. Rep*. **2012**,2,591.
DOI: 10.1038/srep00591
11. Lee M.M.; Teuscher J.; Miyasaka T.; Murakami T.N. and Snaith H.J., *Science*, **2012**, *338*,643-647.
DOI: 10.1126/science.1228604
12. Huang L.; Hu Z.; Xu J.; Sun X.; Du Y.; Ni J.; Cai H.; Li J.; Andzhang J., Solar Energy Materials and Solar Cells, **2016**, *149*, 1-8.
DOI: 10.1016/j.solmat.2015.12.033
13. Ball J.M.; Lee M.M.; Hey A. and Snaith H.J., *Energy Environ. Sci.* **2013**, 1739-1743.
DOI: 10.1126/science.1243167
14. Etgar L.; Gao P.; Xue Z.; Pery Q.; Chandiran A.K.; Liu B.; M.K. and Nazeerudin M.Gratzel , , *J. Am. Chemical Science* **2012**, 134, 17396-17399.
DOI: 10.1021/ja307789s
15. Fang Y. and Huang J.; *Adv. Mater.* **2015**, *27*, 2804- 2810.
DOI: 10.1002/adma.201500099
16. Saidaminov M. I.; Adinolfi V.; Comin R.; Abdehady A. L.; Peng W.; Dursan I.; Yuan M.; Hoogland S.; Sergeant E.H. and Bark O. M., *Nat. Commun.* **2015**, 6, 8724.
DOI: 10.1038/ncomms9724
17. Lidon G. E.; Araceli M. S.; Michele S. and Henk J. B., *J.phys.chem.let.* **2015**, 6, 3743-3749.
DOI: 10.1021/acsJpclett5b01716.
18. Eun J. Y.; Miaogiang L.; Jung-Ho Y.; Chi J. K.; Young J. C. and LianZhou W., *Adv.Mater* **2015**, 27, 6170-6175.
DOI: 10.1002/adma.201502889
19. Gu C. And Lee J. S. *ACS Nano*. **2016**, 10, 5413-5418.
DOI: 10.1021/acsnano.6b01643
20. Deschler F.; Price M.; Pathak S.; Klintberg L.; Jarausch D.D.; Higler R.; Huettner S.; Leijtens T.; Strank S.D.; Snaith H.J. et al. *J. phys. Chem. Lett.,* **2014**, 5, 1421-1426.
DOI: 10.1021/jz5005285
21. D'Innocenzo V.; Srimath kandada A.R.; De Bastiani M.; Gandini M. and Petrozza A. *J.Am.Chem.Soc.,* **2014**, 136 17730-17733.
DOI: 10.1021/ja511198f
22. Luo J.; Im J. H.; Mayer M. T.; Schreier M.; Nazeeruddin M. K.; Park N. G.; Tilley S. D.; Fan H. J.; Grätzel M. *Scien*ce, **2014**, *345*, 1593.
DOI: 10.1126/science.1258307
23. Hoang M. T.; Pham N. D.; Han J. H.; Gardner J. M. and Oh I. *ACS Appl. Mater. Interface* **2016**, *8*, 11904.
DOI: 10.1021/acsami.6b03478

24. Wei H.; Fang Y.; Mulligan P.; Chuirazzi W.; Fang H. H.; Wang C. Ecker B. R.; Gao Y.; Loi M. A.; Cao L. and Huang J., *Nature Photonics* **2016**, 10, 333.
    DOI: 10.1038NPHOTON.2016.41

25. Yakunin S.; Sytnyk M.; Kriegner D.; Shrestha S.; Richter M.; Matt G. J.; Azimi H.; Brabec C. J.; Stany J.; Kovalenko M. V. and Heiss W., *Nature Photonics*, **2015**, 9, 444-449.
    DOI: 10.1038/NPHOTON,2015.82

26. Kojima A.; Teshima K.; Shirai Y.; Miyasaka T., *J. Am. Chem. Soc.* **2009**,131, 6050.
    DOI: 10.1021/ja809598r

27. J.H.; Lee C.R.; Lee J.W.; Park S.W.; Park N.G.; *Nanoscale*, **2011**, 3, 4088.
    DOI: 10.1039/c1nr10867k

28. Zhou H.; Chen Q.; Li G.; Song T.; Duan H.S.; Hong Z.; You J.; Liu Y.; Yang Y. Y., *Science*, **2014**, 345, 542.
    DOI: 10.1126/science.1254050.

29. Research cell efficiency records, NREL 2015
    http://www.nrel.gov/ncpv/image/efficiency chart.jpg

30. Edri E.; Kirmayer S.; Henning A.; Mukhoaphadhyay S.; Gartsman K.; Rasenwaks Y.; Hodes G.; Cahen D., *Nano Lett.* **2014**, 14, 1000.
    DOI: 10.1021/nl404454h

31. Yu H.; Wang F.; Xie F.; Li W.; Chen J. and Zhao N., *Adv. Funct.Mater.* , **2014**, 24, 7102–7108.
    DOI: 10.1002/adfm.201401872

32. Yantara N.; Yanan F.; Shi C.; Dewi H. A.; Pablo P. B.; Subodh G. M. and Mathews N., *chem. Mater.* **2015**, 27, 2309-2314.
    DOI: 10.1021/cm502710r

33. Williams A. E.; Holliman P. J.; Carnie M. J.; David M. L.; Worsley A. and Watson T. M., *J. Mater. Chem. A*, **2014**, 2, 19338-19346.
    DOI: 10.1039/C4TA04725G

34. Glaser T.; Muller C.; Sender M.; Krekeler C.; Esemonin O.; Hull T.D.; Yaffe O.; Owen J.S.; Kowalsky W.; Pucci A. et al *J. Phys. Chem. Lett.,* **2015**, 6, 2913-2918.
    DOI: 10.1021/acs.jpclett.5b01309

35. Theoret A.; Sandorfy C., *Spectrochim. Acta,* **1967**, 23A, 519-542.
    DOI: 10.1016/0584-8539(67)80310-6

36. Antoniadou M.; Siranidi E.; Vaenas N.; Kontos A.G.; Stathatos E. and Falaras P., *J. Surface Interface, Mater.*, **2014**, 2, 323-327.
    DOI: 10.1166/jsim.2014.1060

37. Damma T.; Fourati N.; Boughzala H.; Mlayah A.; Abid Y., *J. Lumin* **2007**, 127, 404-408.
    DOI: 10.1016/j.jlumin.2007.02.001

38. Malalej A.; Abid Y.; Kellel A.; Daoud A.; Lautie A. R., *Solid State Commun.* **1997**, 5, 579-284.
    DOI: 10.1016/S0038-1098(97)00199-3

39. Rao H.; Sun W; Ye S.; Yan W.; Li Y.; Peng H.; Liu Z.; Bian Z. and Huang C., *ACS Appl. Mater. Interfaces*, **2016**, 8, 7800-7805.
    DOI: 10.1021/ascami.5b12776

40. Liu Y.; Renna A.; Page Z. A.; Kim P.; Choi J.; Emrick T.; Vankataraman D. and Russell T. P, *ACS Appl. Mater. Interfaces*, **2016,** 8, 7070-7076.
    DOI: 10.1021/acsami.5b12740

41. Shao F.; Xu L.; Tian Z.; Wang Y.; Sheng P.; Wang D. and Huang F., *RSC Adv.***2016**, 6, 42377-42382.
    DOI: 10.1039/c6ra05718g

42. Singh T.; Singh J. and Miyasaka T., *ChemSusChem,* **2016**, 9, 1 – 9.
    DOI: 10.1002/cssc.201601004

43. Dursun I.; Shen C.; Pride M. R.; Pan J.; Sarmah S. P.; Priante D.; Alyani N.; Liu J.; Saidaminov M. I.; Alias M. S.; Mohammed O. F.; Ooi B. S. and Bakr O. M., *Acs Photonics* **2016**, *3,* 1150–1156.
    DOI: 10.1021/acsphotonics.6b00187

44. Xia H. R.; Sun W.T. and Peng L. M. *Chem. Commun.* **2015**, 51, 13787.
    DOI: 10.1039/c5cc05053g

45. Liu J.; Xue Y.; Wang Z.; Xu Z.; Zheng C.; Weber B.; Song J.; Wang Y.; Lu Y.; Zhang Y. and Bao Q. L., *Acs Nano,* **2016,** 10, 3536-3542.
    DOI: 10.1021/acsnano.5b07791